Theor Chim Acta (1989) 76: 353–371

Theoretica Chimica Acta

A systematic treatment of three-dimensional quantum mechanical reaction coordinates

Norman M. Witriol[1] and Gary H. Herling[2]

[1] Naval Research Laboratory, Washington, DC 20375-5000, and Department of Physics, Louisiana Tech. University, Ruston, LA 71270, USA,

[2] Naval Research Laboratory, Washington, DC 20375-500, USA

(Received March 7; revised and accepted July 14, 1989)

Summary. The rigorous, collinear, canonical point transformation method with "hyper-hyperbolic" coordinates is extended to the infinite central mass problem in three dimensions. The initial transformation performed is $(x_A, y_A, z_A, x_C, y_C, z_C) \rightarrow (\phi, \theta, \psi, r, R, \tau)$, where (ϕ, θ, ψ) are the Euler angles; r and R are the AB and BC interatomic distances, respectively, and τ is the angle between $\boldsymbol{r}$ and $\boldsymbol{R}$. A second transformation is then performed to $(\phi, \theta, \psi, \xi, \eta, \tau)$, where ξ is the reaction coordinate mimicking the reaction path, and η is the vibrational coordinate of the diatom. The transformed spaces are all one-to-one mappings from the original spaces, and thus do not have any three-to-one regions. The transformed momenta and Hamiltonians are derived, and are Hermitian in their respective transformed spaces.

Key words: Reactive scattering — Reaction coordinates — Molecular scattering

1. Introduction

In recent years, with the advent of and access to supercomputers, there has been a resurgence of theoretical consideration of three-dimensional reactive processes. Recent calculations have employed $\mathscr{L}^2$ basis sets and non-local interactions which couple different arrangement channels [1, 2], hyperspherical coordinates [3, 4], matching surfaces [5], and natural collision coordinates with matching surfaces [6, 7]. The present work is concerned with an attempt to implement the reaction path concept [8] in three-dimensional (3D) quantum mechanical calculations of atom-diatom reactive scattering. The stationary phase approximation to the path integral formulation of quantum mechanics [9] indicates that the largest

contributions to the transition amplitude arise in the vicinity of classical orbits. Consequently, a coordinate system based on the classical reaction path might be expected to be computationally advantageous.

Motion in terms of the reaction coordinate may be considered to be a large amplitude excursion corresponding to the imaginary frequency at the potential saddle point [10]. For the infinite central mass case considered in the present work, modified heliocentric coordinates [11] might be expected to be useful, but their utility is limited by the magnitude and complexity of their induced changes in the form of the potential. Orthogonal relative coordinates [12] have, in common with the body-fixed coordinates of the present work, the properties that the "radial coordinates" are orthogonal to each other and *all* of the angular coordinates, but the body-fixed angular coordinate is not orthogonal to the Euler angles. Both of these systems, however, have been advocated for bound state problems rather than scattering problems.

The reaction path, ξ_p, is the path of steepest descent in mass weighted coordinates extending from the potential saddle point to the reactant and product valleys. As described by Light [13], the reaction curve, ξ_c, is an *ad hoc* curve chosen to mimic the reaction path, ξ_p. The curve is parameterized in such a manner that, as the reaction proceeds, the reaction coordinate, ξ, goes from $-\infty$ to $+\infty$. The asymptotic reactant and product regions are thus described by the same Hamiltonian, thereby avoiding (i) the "scrambling" of continuum and bound coordinates which otherwise occurs in the reaction region, and (ii) projective procedures, which are sometimes used in perturbative rate methods [14]. As in activated complex theory, the reaction coordinate concept allows visualization of the actual reaction path in terms of a single coordinate, ξ. In addition, dynamical analysis in the reaction coordinate picture, which has been shown to reduce to activated complex theory in the relevant statistical limit [15], easily incorporates the intuitive notions concerning the location and shape of energy barriers, which are powerful concepts in the absolute rate theory formulation.

In an earlier paper [16] on this method, henceforth referred to as I, the collinear triatomic collision problem was considered, and a family of "hyper-hyperboloids" comprising an orthogonal set of coordinates was found. One of the coordinates, ξ, mimics the reaction path, ξ_p; the other coordinate, η, being orthogonal to ξ, describes, in the asymptotic regions, the vibrational states of both the reactant and the product systems. The transformation employed was simply a point transformation, and thus no mathematical ambiguities, or physically meaningless artifacts were used. Because the point transformation is global, the method was well able to handle the "centrifugal" force, or "bobsled" effects [17] in reactive or nonreactive collisions, wherein the point representing the average position of the system leaves the reaction path because of its curvature. This effect is extremely important because the departure of the reaction from the reaction path describes the vibrational excitation of the system (both reactant and product) and thus is essential in obtaining the propensity rules [15, 18] for the reaction. In previous methods, following the earlier work of Marcus [17, 19] and Child [20], the curves were taken to be straight line extensions of local

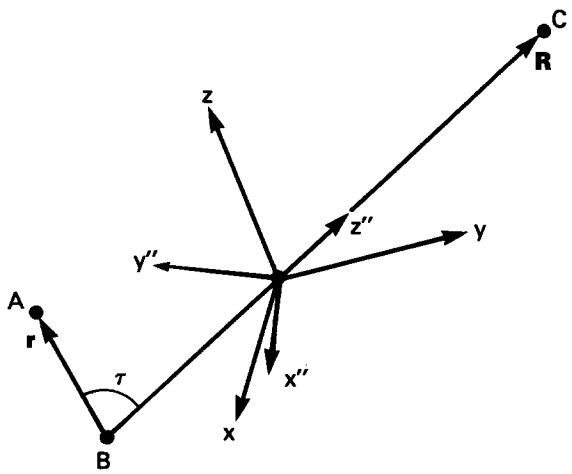

Fig. 1. Space-fixed axes (x, y, z) and body-fixed axes (x'', y'', z'') for the entrance channel of the reaction $AB + C \rightarrow A + BC$. Although the origin of the coordinates is at B, it has been displaced from that point for the sake of clarity in the figure. The space-fixed areas are arbitrary. In the body-fixed system, the z''-axis points from atom B to atom C while the y''-axis is normal to the reaction plane in the $\boldsymbol{r} \times \boldsymbol{R}$ direction

perpendiculars to the reaction curve, ξ_c. At large curvatures, with energies sufficient to appreciably depart from the reaction path, or if tunneling were taken into consideration, dynamical calculations in the triple valued regions where the local perpendiculars could cross were impossible.

The "hyper-hyperbolic" coordinates introduced in I were one-to-one over the whole space, and thus entirely eliminated this problem. The point transformation method transforms the coordinates, momenta, Hamiltonian, and wave functions together. The transformation is always orthogonal in the transformed space, while the momenta and Hamiltonian are Hermitian. No approximations are used; the Hamiltonian is exact. McNutt and Wyatt [21] extended the method developed in I to the finite mass case. In doing so, they transformed the differential equation to a form more amenable to computational solution.

In this paper, the extension to the three-dimensional problem of the infinite mass case method developed in I is considered. For the A–B–C system, with $M_B = \infty$, and with the origin of the coordinate system chosen to be at B, the original coordinates, shown in Fig. 1, are $(x_A, y_A, z_A, x_C, y_C, z_C)$. An initial transformation to the variables $(\phi, \theta, \psi, r, R, \tau)$ is performed; here (ϕ, θ, ψ) are the Euler angles, r and R are the interatomic distances r_{AB} and r_{BC}, respectively, and τ is the angle between $\boldsymbol{r}$ and $\boldsymbol{R}$. A second transformation to the variables $(\phi, \theta, \psi, \xi, \eta, \tau)$ where ξ is the reaction coordinate, and η is the vibrational coordinate of the diatomic system produces the final result. Section 2 is concerned with these transformations. The transformation of the momenta and Hamiltonian is discussed and compared with the results of [5] in Sect. 3, while Sect. 4 contains concluding remarks. The elements of the 6×6 matrix of first derivatives of the intermediate variables with respect to the original variables comprise Appendix A, and the proof that two successive point transformations are equivalent to a single transformation appears in Appendix B.

2. The transformation

Consider the infinite central mass A–B–C reactive collision problem as shown in Fig. 1. Following the standard methods, one transforms to a barycentric reference frame with the origin on the infinite mass atom B. The space-fixed barycentric coordinates are then $(x_A, y_A, z_A, x_C, y_C, z_C)$. Applied to the reaction path, the point transformation method transforms to a set of coordinates which are analytic, form a one-to-one mapping of the space, and have one which mimics the actual reaction path as closely as possible.

An initial transformation is performed to body-fixed coordinates by introducing Euler angles of the A–B–C system (ϕ, θ, ψ), the interparticle distances, $r = r_A$, and $R = r_C$, and the angle between $\boldsymbol{r}$ and $\boldsymbol{R}$, τ. In order to enable the introduction of the helicity representation for a partial wave decomposition of the wave function, the first two Euler angle rotations are chosen to orient the body-fixed z-axis to point from atom B, the diatom center of infinite mass, to the lone atom in each channel. For the incoming channel, as shown in Fig. 1, the final z-axis, z'', is in the $\boldsymbol{R}$ direction. The final rotation angle, ψ, orients the final y-axis, y'', in the $\boldsymbol{r} \times \boldsymbol{R}$ direction normal to the atom-diatom plane. The Euler angles [22] for this transformation are then given by

$$\phi = \tan^{-1}(y_C/x_C) + \alpha,$$
$$\theta = \cos^{-1}(x_C/R),$$

and

$$\psi = \tan^{-1}\left(\frac{n_z R}{x_C n_y - y_C n_x}\right) + \beta, \tag{2.1}$$

where R is the B–C interparticle separation, $R = (x_C^2 + y_C^2 + z_C^2)^{1/2}$, $\boldsymbol{n}$ is the perpendicular to the A–B–C plane,

$$\boldsymbol{n} = \boldsymbol{r} \times \boldsymbol{R}, \tag{2.2}$$

and $n = |\boldsymbol{n}|$. The quantities α and β are included for computational purposes, and are defined as follows:

$$\begin{aligned} \alpha &= 0, \quad n_x, n_y \geqslant 0; & \beta &= 0, \quad z_C n, \quad \Delta \geqslant 0 \\ &= 2\pi, \quad n_x < 0, \quad n_y > 0; & &= 2\pi, \quad z_C n < 0, \quad \Delta > 0 \\ &= \pi; \quad \text{otherwise}; & &= \pi, \quad \text{otherwise}, \end{aligned} \tag{2.3}$$

where

$$\Delta = n_x y_C - n_y x_C. \tag{2.4}$$

These Euler angles are channel dependent and therefore lack the appeal of the reaction path concept, *viz.*, both the entrance and exit channels are described by the same Hamiltonian. Another set of Euler angles wherein the first two rotations orient the z-axis in the direction perpendicular to the reaction plane, with the third Euler angle orienting the y-axis in the atom-diatom direction may

be defined. This set has the advantage that only one angle is channel dependent. However, its disadvantage is that one cannot readily separate out the orbital angular momentum, $\boldsymbol{l}$, and the standard wave function decompositions become difficult. This orientation has been employed in formulations of the three-body problem in terms of hyperspherical coordinates [23, 24], but it leads to difficulties in the formulation of coupled-state equations [4b].

The other three coordinates, in the infinite mass B case, are taken to be the A–B and the B–C interparticle distances, r and R respectively, and the angle between $\boldsymbol{r}$ and $\boldsymbol{R}$, τ, where

$$\tau = \cos^{-1}\left(\frac{\boldsymbol{r}\cdot\boldsymbol{R}}{rR}\right). \tag{2.5}$$

The goal of the reaction coordinate method is to have one coordinate, ξ, which, while mimicking the reaction path as closely as possible, smoothly proceeds from the reactant to the product region while the other coordinates are perpendicular to it. A transformation which achieves this result for the collinear problem was developed in I. The collinear transformation transformed the two one-dimensional interparticle distances, x_A and x_C, into the reaction coordinate, ξ, and the vibrational coordinate, η. For the three-dimensional problem, one must also consider the angle, τ. For the $H_2 + F \rightarrow H + HF$ reaction, the reaction path is collinear [25] and lies in the $\tau = \pi$ plane. The reaction coordinate is, therefore, chosen to be explicitly independent of τ. For other cases, the angular dependence of the reaction path may be quite complicated, and is generally not known analytically. In such cases, for which the potential surface admits of reactive pathways for a broad range of τ, it is nevertheless convenient to choose the reaction coordinate to be independent of τ. In particular, the same point transformation as in the collinear case is used to transform the interparticle distances, r and R, into ξ and η. From I Eqs. (4.11) and (4.12), the transformation is

$$\begin{aligned} \xi &= r^4 - R^4, \\ \eta &= \frac{rR}{r^2 + R^2} - \eta_0, \end{aligned} \tag{2.6}$$

or more generally,

$$\begin{aligned} \xi &= (bR + R_0)^4 - (ar + r_0)^4, \\ \eta &= \left[\frac{(ar + r_0)^2(bR + R_0)^2}{a^2(ar + r_0)^2 + b^2(bR + R_0)^2}\right]^{1/2} - \eta_0 \end{aligned} \tag{2.7}$$

for all values of τ.

Thus, from Eqs. (2.1), (2.5) and (2.7), there is a six-dimensional point transformation, which provides a one-to-one mapping of the space-fixed coordinates onto the Euler angles, (ϕ, θ, ψ), and three reaction coordinates, (ξ, η, τ) which respectively represent translation, vibration, and rotation in both the reactant and product channels of this single product reaction.

3. The transformed Hamiltonian

Having given the transformation, the point transformation method [26, 27] may be applied to the calculation of the Hamiltonian, and the wave function in the transformed space. The method is substantially different from simply performing a change of variables. The variables in the transformed space are orthogonal, the transformed momenta are not simply given by the chain rule, and thus the transformed Hamiltonian and wave function are not the same as the original Hamiltonian and wave function written in terms of the transformed variables. At the end of this section these results will be briefly compared with those obtained from the change of variables method, the method wherein the chain rule for differentiation is used, and thus one remains in the original space.

The point transformation, given by Eqs. (2.1), (2.5) and (2.7) can be compactly written in the form

$$\boldsymbol{\eta} = \boldsymbol{\eta}(\boldsymbol{x}), \tag{3.1}$$

where $\boldsymbol{\eta} = (\phi, \theta, \psi, \xi, \eta, \tau)$ and $\boldsymbol{x} = (x_A, y_A, z_A, x_C, y_C, z_C)$. The relationship between the original momenta P_i (conjugate to x_i) and the transformed momenta, p_i (conjugate to η_i) is taken to be

$$P_i = (1/2) \sum_{j=1}^{6} [(\partial \eta_j / \partial x_i) p_j + p_j (\partial \eta_j / \partial x_i)], \tag{3.2}$$

where, in the coordinate representation of the original space,

$$P_i = i\hbar \, \partial / \partial x_i, \tag{3.3}$$

and in the coordinate representation in the transformed space,

$$p_j = -i\hbar \, \partial / \partial \eta_j. \tag{3.4}$$

From Eqs. (3.3) and (3.4), it is seen that Eq. (3.2) is not the chain rule for differentiation. This difference is the reason [26] that the transformed variables in the transformed space are orthogonal, with well-defined momenta given by Eq. (3.4). The original Hamiltonian, in the infinite mass B case, is given by

$$H = (1/2) \sum_{i=1}^{6} (P_i^2 / m_i) + V(x), \tag{3.5}$$

where $\boldsymbol{x} = (x_A, y_A, z_A, x_C, y_C, z_C)$, and $m_i = m_A$ for $i = 1-3$ and $m_i = m_B$ for $i = 4-6$. Proceeding to mass weighted coordinates,

$$x_A \rightarrow (m_A)^{1/2} x_A, \qquad x_C \rightarrow (m_C)^{1/2} x_C, \tag{3.6}$$

and similarly for y and z, the original Hamiltonian, given by Eq. (3.5), becomes

$$H = (1/2) \sum_{i=1}^{6} P_i^2 + V(\boldsymbol{x}). \tag{3.7}$$

The transformed Hamiltonian obtained via the standard canonical procedure [26] is given by

$$H[\boldsymbol{x}(\boldsymbol{\eta}), \boldsymbol{P}(\boldsymbol{\eta}, \boldsymbol{p})] = (1/2) \sum_{i,j=1}^{6} p_i g^{ij} p_j + W(\boldsymbol{\eta}) + V(\boldsymbol{\eta}), \tag{3.8}$$

where g^{ij} is the effective metric,

$$g^{ij} = \sum_{k=1}^{6} (\partial \eta_i / \partial x_k)(\partial \eta_j / \partial x_k), \tag{3.9}$$

$W(\boldsymbol{\eta})$ is the coordinate dependent potential,

$$W = (\hbar^2/2) \sum_{i,j=1}^{6} B^{1/2}(\partial/\partial \eta_i) g^{ij}(\boldsymbol{\eta})(\partial/\partial \eta_j) B^{-1/2}, \tag{3.10}$$

or, in terms of the original coordinates (sometimes a more convenient calculation),

$$W = -(\hbar^2/2) \sum_{k=1}^{6} (\partial/\partial x_k)(B^{-1/2}\, \partial B/\partial x_k), \tag{3.11}$$

in which B is the Jacobian of the inverse transformation, $\boldsymbol{\eta} \rightarrow \boldsymbol{x}$,

$$B = |\partial \eta_j / \partial x_i|, \tag{3.12}$$

and $V(\boldsymbol{\eta})$ is simply $V(\boldsymbol{x})$ written in terms of the transformed variables. The relationship [26, 27] between the wave function, $\Psi(\boldsymbol{x})$, in the original space, and the wave function, $\Psi(\boldsymbol{\eta})$, in the transformed space, is

$$\Psi(\boldsymbol{x}) = B^{1/2} \Psi(\boldsymbol{\eta}). \tag{3.13}$$

This relationship guarantees [26, 27] that the time-independent Schrödinger equation is of the same form in both the original and transformed spaces. As one can readily see, it also guarantees conservation of probability with a weight function of one in the transformed space which is consistent with the orthogonality of the transformed variables in the transformed space.

In various guises, Eqs. (3.8) and (3.13) have a venerable history [26–30]. Different conventions for the metric have been used, but that of the present work is the same as that of [28]. The emphasis of the earlier work [28–30] was focussed on the correct transcription of a classical Hamiltonian into a Schrödinger equation with the same coordinates; this is equivalent to the transformation of the Laplacian to generalized curvilinear coordinates. The more recent work has focussed on the transformation of the quantum mechanical coordinates and momenta themselves as the result of a classical canonical point transformation. Both approaches lead to exactly the same results provided that the Jacobian factors needed for the normalization integral [26–30] are consistently taken into account. The separation of Eq. (3.8) into a term quadratic in the momenta and an induced potential, W, manifests the similarity between the classical and quantum mechanical Hamiltonians. The potential W, which arises solely as a result of the coordinate transformation, is proportional to $\hbar^2$ and vanishes in the classical limit.

The effect of the transformation, indicated by the subscript 1, from the space-fixed coordinates to the body-fixed coordinates $\eta_1 = (\phi, \theta, \psi, r, R, \tau)$ is first considered. In order to obtain the Hamiltonian in the transformed coordinates, H_1, (given by Eq. (3.8) with W, η, and g^{ij} replaced by W_1, η_1, and g_1^{ij}, respectively it was first necessary to obtain the derivatives, $\partial\eta_{1j}/\partial x_i$, of the transformation given by Eqs. (2.1) and (2.5). The effective metric coefficients, g_1^{ij}, and the coordinate dependent potential W_1 were then calculated. The algebraic manipulations were performed with the symbolic manipulation program SMP [31] on a VAX 780/11 computer. The derivatives, $\partial\eta_{1j}/\partial x_i$ are given in Appendix A. Using Eq. (3.9) with η replaced by η_1, the independent effective metric coefficients g_1^{ij}, are then found to be

$$
\begin{aligned}
&g_1^{11} = (R \sin\theta)^{-2},\\
&g_1^{12} = 0,\\
&g_1^{13} = -(\cos\theta \sin\tau + \cos\psi \cos\tau \sin\theta)(R \sin\theta \sin\tau)^{-2},\\
&g_1^{14} = g_1^{15} = 0,\\
&g_1^{16} = -\sin\psi(R^2 \sin\theta)^{-1},\\
&g_1^{22} = R^{-2},\\
&g_1^{23} = \cos\tau \sin\psi(R^2 \sin\tau)^{-1},\\
&g_1^{24} = g_1^{25} = 0,\\
&g_1^{26} = -\cos\psi R^{-2},\\
&g_1^{33} = (r \sin\tau)^{-2} + (R \sin\tau)^{-2} + (R \sin\theta)^{-2} - 2R^{-2}\\
&\qquad + 2\cos\psi \cos\tau \cos\theta(R^2 \sin\tau \sin\theta)^{-1},\\
&g_1^{34} = g_1^{35} = 0,\\
&g_1^{36} = \cos\theta \sin\psi(R^2 \sin\theta)^{-1},\\
&g_1^{4j} = \delta_{4j}, \quad j = 4, 5, 6,\\
&g_1^{5j} = \delta_{5j}, \quad j = 5, 6,\\
&g_1^{66} = r^{-2} + R^{-2}.
\end{aligned}
\tag{3.14}
$$

The Jacobian of the inverse initial transformation, as in Eq. (3.12), is

$$B_1 = -(r^2 R^2 \sin\tau \sin\theta)^{-1}. \tag{3.15}$$

Substituting Eqs. (3.14) and (3.15) into Eq. (3.10) yields the induced coordinate dependent potential for the initial transformation,

$$
\begin{aligned}
(2/\hbar^2)W_1(\eta) = &-(2r \sin\tau)^{-2} - (2R \sin\tau)^{-2} - (2R \sin\theta)^{-2} - (2r)^{-2}\\
&- (2R^2)^{-1} + \cos\psi \cos\tau \cos\theta(2R^2 \sin\tau \sin\theta)^{-1}.
\end{aligned}
\tag{3.16}
$$

Equation (3.8), together with Eqs. (3.11)–(3.14), constitutes the Hamiltonian for the initial transformation to body-fixed coordinates.

The second transformation, $(\theta, \psi, r, R, \tau) \rightarrow (\phi, \theta, \psi, \xi, \eta, \tau)$, as given by Eq. (2.7) and indicated by the subscript 2, transforms to the reaction coordinates, (ξ, η). As with the initial transformation, it is necessary to obtain the derivatives, $\partial \eta_{2j}/\partial x_i$, of the transformation of Eq. (2.7), and calculate the effective metric g^{ij} and the coordinate dependent potential, W_2. The method for combining two successive transformations is given in Appendix B. The effective metric, Eq. (B.9), does not contain a subscript because the final form for g is not simply additively or multiplicatively related to g_1 and g_2. Because the transformation of Eq. (2.7) only involves two of the six coordinates, only a two by two submatrix of the derivatives is affected. Setting $x = ar + r_0$ and $y = bR + R_0$, one obtains

$$\begin{aligned}
&\partial \eta_{2i}/\partial \eta_{ij} = \delta_{ij}, \qquad i \neq 4, 5; \quad j \neq 4, 5, \\
&\partial \eta_{24}/\partial \eta_{14} = -4ax^3, \\
&\partial \eta_{24}/\partial \eta_{15} = 4by^3, \\
&\partial \eta_{25}/\partial \eta_{14} = ab^2y^3[(ax)^2 + (by)^2]^{3/2}, \\
&\partial \eta_{25}/\partial \eta_{15} = ba^2x^3[(ax)^2 + (by)^2]^{3/2}.
\end{aligned} \tag{3.17}$$

Similarly, only a two by two submatrix of g^{ij} is affected, namely,

$$\begin{aligned}
&g^{ij} = g_1^{ij}, \qquad i, j \neq 4, 5, \\
&g^{44} = 16(a^2x^6 + b^2y^6), \\
&g^{45} = g^{54} = g_1^{45} = 0, \\
&g^{55} = (ab)^2(a^2x^6 + b^2y^6)[(ax)^2 + (by)^2]^{-1}.
\end{aligned} \tag{3.18}$$

The Jacobian of the inverse transformation is given by

$$B_2 = 4ab(a^2x^6 + b^2y^6)(rR)^{-2}[(ax)^2 + (by)^2]^{-3/2}, \tag{3.19}$$

and the final Jacobian is the product of the two Jacobians B_1 and B_2,

$$B = B_1 B_2 = 4ab(a^2x^6 + b^2y^6)(rR)^{-2}(\sin\theta \sin\tau)^{-1}[(ax)^2 + (by)^2]^{-3/2}. \tag{3.20}$$

The final effective potential is given by

$$W = W_1 + W_2, \tag{3.21}$$

where W_1 is given by Eq. (3.16) and apart from the factor $\hbar^2/2$

$$\begin{aligned}
W_2 = (3/4)\{&(ab)^6[(ax)^2(28x^8y^4 - 2x^{12} + 5y^{12}) + (by)^2(28x^4y^8 + 5x^{12} - 2y^{12}) \\
&+ a^2b^4y^6(18a^8x^8 + b^8y^8 + 2a^2b^6x^2y^6 + 24a^6b^2x^6y^2) + a^4b^2x^6(a^8x^8 + 18b^8y^8 \\
&+ 24a^2b^6x^2y^6 + 2a^6b^2x^6y^2)]\}[((ax)^2 + (by)^2)(ab^3y^6 + a^3bx^6)]^{-2}.
\end{aligned} \tag{3.22}$$

Equation (3.8) coupled with Eqs. (3.16), (3.18), (3.21), and (3.22) constitute our basic result: the transformed Hamiltonian of the system. The transformed Hamiltonian and the transformed momenta are Hermitian. Both the transformed wave function and the transformed Hamiltonian are given in terms of the transformed variables, and are taken in the transformed space.

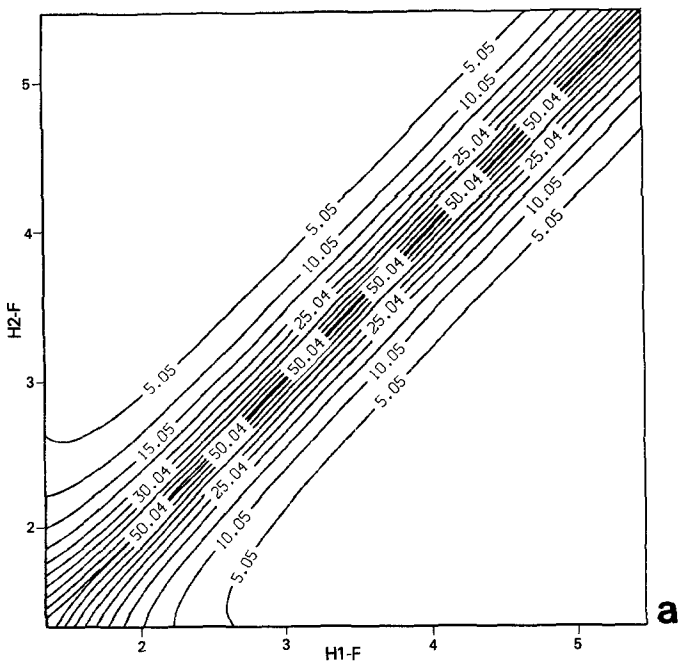
H2-F
H1-F
5.05
10.05
25.04
50.04
15.05
30.04
a

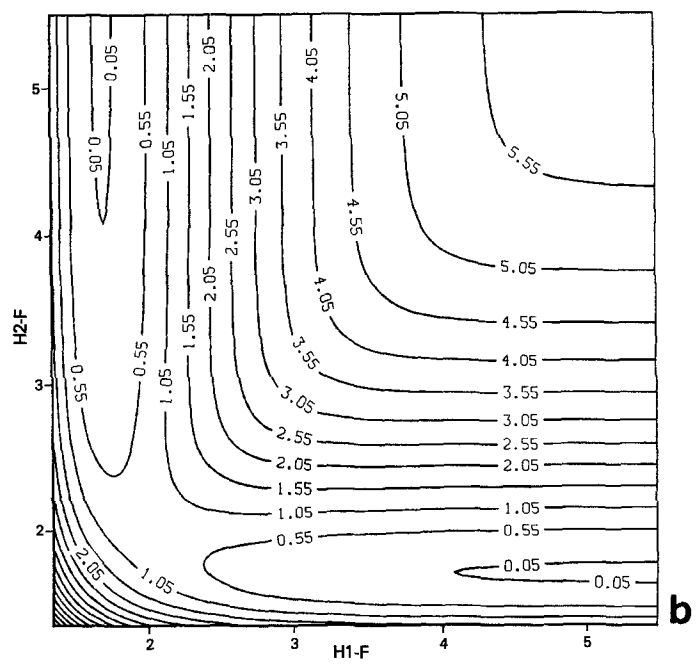
H2-F
H1-F
0.05
0.55
1.05
1.55
2.05
2.55
3.05
3.55
4.05
4.55
5.05
5.55
b

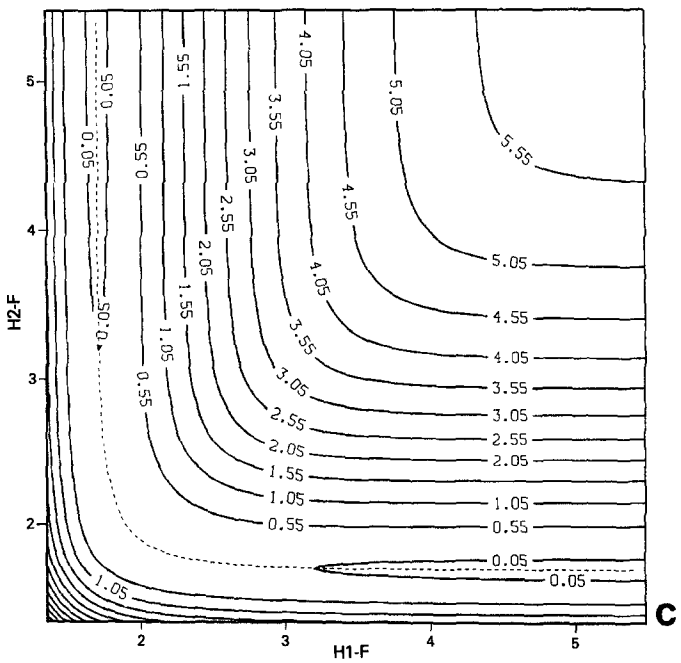

Fig. 2. The Muckerman V [34] potential surface in the $H + FH \rightarrow HF + H$ channel: **a** $\tau = 0$; **b** $\tau = \pi/2$; **c** $\tau = \pi$. The last is the projection that contains the predicted linear transition state for this reaction, [38] and the reaction path is indicated by the *dashed line*

The reaction $H_2 + F \rightarrow HF + H$ has been extensively studied both experimentally and theoretically [25, 32, 33]. Several potential energy surfaces have been proposed for it and employed for classical, semi-classical, and quantum mechanical analyses. The Muckerman V (M-V) surface [34] has apparently become the "surface of choice" for both 1D (one-dimensional) [32] and 3D (three-dimensional) quantum mechanical calculations for this reaction [7, 35, 36], as well as for calculations on $HF + H \rightarrow H + FH$ with hyperspherical coordinates [37]. Consequently, the M-V surface has been chosen for the purpose of illustrating these results for this reaction.

The system approximates the infinite mass central atom B(F) case, and since the binding energy of H_2, 4.5 eV, is much less than that of HF, 6.4 eV, the A-C(H_2) channel can approximately be ignored. A plot of this surface in the (r, R, τ) subspace, for fixed values of τ, is shown in Fig. 2. Figure 2a is a contour map of the surface for $\tau = 0$. In the convention of the present work, $\tau = 0$ corresponds to the approach of one H atom to the other. The repulsive potential indicates that this conformation presents a high barrier for reaction. The map for $\tau = \pi/2$ in Fig. 2b suggests that reaction can take place in the perpendicular configuration. The H–F–H collinear arrangement occurs for $\tau = \pi$ in the map of Fig. 2c. This contains the collinear transition state for the exchange reaction that is predicted by the Muckerman V potential surface, [38] and the reaction path is shown by the dashed line.

Plots of the one-dimensional contours with parameters fitted to the H–F–H system, are given in Fig. 3. The solid lines are curves of constant η, where $\eta = 0$ corresponds to the best fit to the reaction path, while the dashed curves are curves of constant ξ. Throughout all space, the (ξ, η)-coordinate system remains orthogonal. Figure 4 shows how well the reaction coordinate, ξ, can be fitted to the reaction path ξ_p, for the Muckerman V potential energy surface in (r, R) space. The fit is reasonable in the reaction region, and excellent in the asymptotic regions. From the shape of the reaction path, ξ_p, one would not expect to get an excellent fit in the reaction region with a relatively simple analytic function. A plot of the reaction path, ξ_p, in (ξ, η) space is shown in Fig. 5. In their own space, the coordinates ξ and η are rectilinear and orthogonal and the reaction path is depicted by the dashed curve. The values are, of course, numerically equal to the residuals obtained from the best fit to the path. This figure may also be considered as a redrawing of Fig. 4 in the transformed space.

In Fig. 6, the reaction coordinates in a 3D r-R-τ space where τ represents the rotation are plotted. The dotted circles corresponding to fixed (ξ, η) illustrate rotation. The general nature of the point transformation method [26, 27] is such that the transformed variables are orthogonal, and the weight function in the volume integral is one. Because the curves shown in Fig. 6 for constant η and τ are plotted on the orthogonal (r, R)-axes, the figure illustrates the result of a change of variables, not a point transformation. Because the point transformation gives orthogonal variables, an alternative plot of the (r, R, τ) subspace is given in Fig. 7. It shows that constant ξ correctly describes vibration in both the reactant and product channels. However, inspection of Fig. 2 reveals that the plane $\tau = 0$ enters a physically inaccessible region of space. This corresponds to the fact that atoms A and C cannot be at the same point, i.e., if without mass weighting $r = R$, then τ cannot be zero.

The Eulerian transformation, Eq. (2.1), can be utilized within the change of variables concept by performing a standard change of variables using the chain rule. While this method does not yield Hermitian momenta in the Euler angles, etc., it is the standard method currently used. If that method were used, the resultant Hamiltonian would not have the coordinate dependent potential, W_1. The first transformation would yield the Hamiltonian obtained by Schatz and Kupperman [5] which can be written in the form

$$H = \sum_{i,j=1}^{6} \left\{ p_i g^{ij} p_j + \sum_{k=1}^{6} (\partial \eta_{1i}/\partial x_k)(\partial/\partial \eta_{1i})(\partial \eta_{1j}/\partial x_k) \right] p_j \right\} + V(\boldsymbol{\eta}_1), \quad (3.23)$$

where the g^{ij}'s are the effective metric coefficients given by Eq. (3.15), and the $\partial \eta_{1j}/\partial x_k$ are given in Appendix B. The second transformation transforms this Hamiltonian to

$$H = \sum_{i,j=1}^{6} p_i g^{ij} p_j + W_2 + V(\boldsymbol{\eta}_2). \quad (3.24)$$

Because this method is more closely related to the standard methodology, it might be easier to employ computationally than the formal method previously derived.

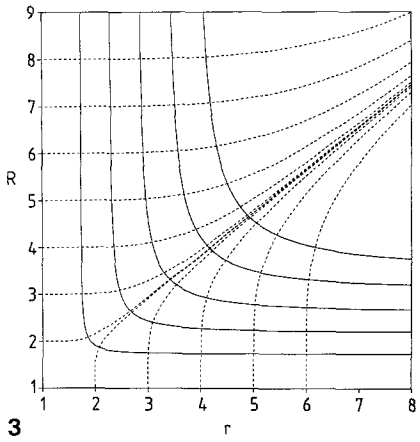

3

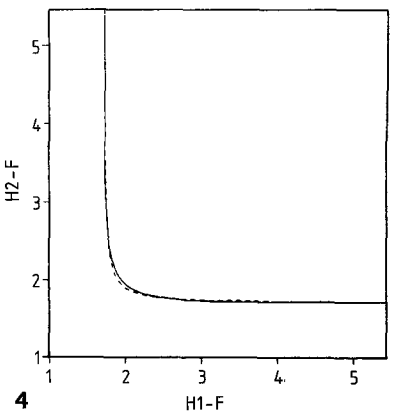

4

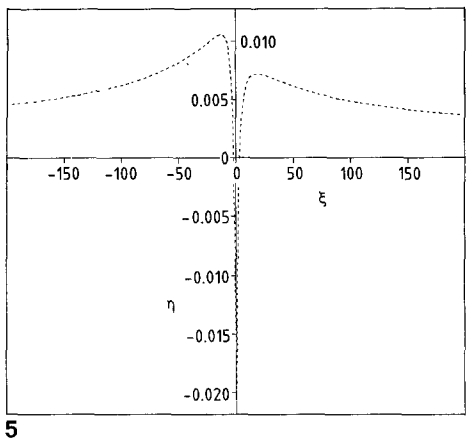

5

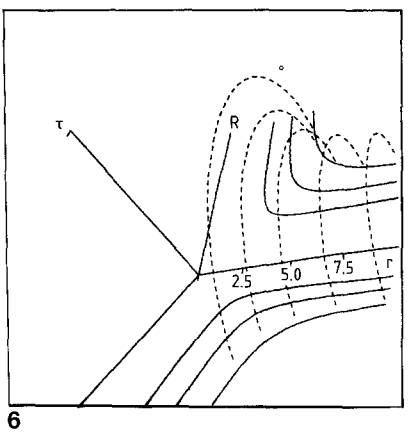

6

Fig. 3. The (ξ, η) coordinates in any plane $\tau =$ constant. The *solid* (*dashed*) *lines* are curves of constant $\eta(\xi)$. They are orthogonal and single valued at every point

Fig. 4. The reaction path and the best fit to it are given by the *solid* and *dashed curves*, respectively, as functions of $R_{H,F}$. The fit is excellent in the asymptotic regions, and reasonable in the reaction region. A value $\chi^2 = 0.01$ was obtained for fitting 174 data points with two parameters

Fig. 5. The reaction path for the Muckerman V potential plotted in (ξ, η) space. The values shown are, in fact, the residuals of the fit to the reaction path

Fig. 6. The (ξ, η, τ) coordinates in (r, R, τ) space. For clarity, the curves of constant ξ have been omitted. The *solid lines* are values of constant ξ, and the angle τ corresponds to the rotations indicated by the *dashed lines*

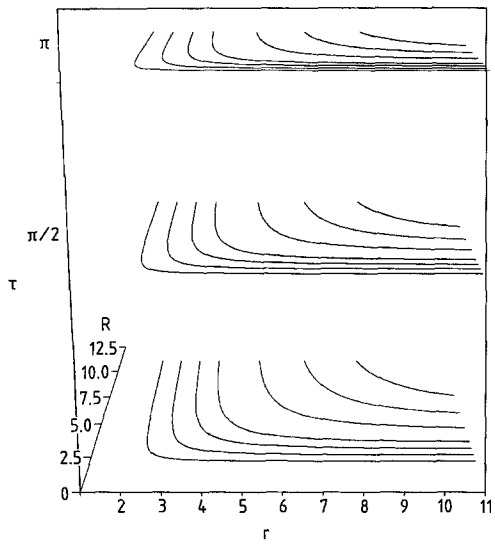

Fig. 7. Another representation of the three-dimensional (ξ, η, τ) coordinates in (r, R, τ) space. The curves of constant ξ have been omitted for clarity, and the "z"-axis corresponds to the angle τ

The reason that the formal method of performing the transformation from space fixed to body fixed is more difficult to implement computationally is that it leads to the coordinate dependent potential W_1 given by Eq. (3.16). This not only contains singularities, but also couples the dynamical variables of the problem to the geometric Euler angles. In the usual partial wave decomposition, a more complicated set of coupled equations is, therefore, expected. Even if W_1 were eliminated from the problem, rotation in the three-dimensional problem leads to additional computational difficulty. Although a convenient ξ-dependent vibrational basis may be easily constructed, and has been for the collinear problem [21], rotations present difficulties. The construction of a reaction coordinate dependent rotational basis has been performed [7], but it requires additional matrix diagonalizations. It appears, therefore, that it is formally possible to reduce the three-dimensional problem to a set of coupled ordinary differential equations in the reaction coordinate for the translational functions similar to that of [21]. Equations of the same form have been derived under the more restrictive assumption that the "surface functions" multiplying the translational functions are independent of the scattering coordinate [39].

4. Conclusions

In this paper the extension of the reaction coordinate point transformation method to the three-dimensional quantum mechanical reactive scattering problem has been considered. In Sect. 2, the transformation to the incoming channel Euler angles was described. The collinear reaction coordinate transformation was appended to the Euler angle transformation, thereby completing the three-dimensional reaction coordinate transformation. It was found that the point transfor-

mation proceeded smoothly, and no procedural or computational difficulties were encountered. However because the axes defining the Euler angles are different in different channels, the formulation lacks the intuitive appeal of the Polanyi concept wherein a given coordinate represents the same physical variable in both the incoming and the outgoing channels. Extensions of this method by means of smoothing cutoff functions [40] to manifest this behavior have been considered, but they introduce problems in the basis set expansion of the wave function. Nevertheless this technique might bear further investigation.

For the current work, the integration techniques in the transition-state region may be significantly simpler than those of [5] because the reaction coordinates automatically take curvature into account, and thus there is no need to introduce arbitrary and changing propagation coordinates. In addition the matching appears to be simpler because the vibrational and translational coordinates are the same across the matching boundary. No approximations pertaining to the harmonicity of the potential in certain variables, or to cutoffs to avoid triple-valued regions, have been incorporated. The collinear "hyper-hyperbolic" reaction coordinate method has thus been extended to the consideration of three-dimensional problems.

Appendix A

The derivatives $\partial\eta_{1j}/\partial x_i$, *where* $\boldsymbol{\eta}_1 = (\phi, \theta, \psi, r, R, \tau)$ *and* $\boldsymbol{x} = (x_A, x_C, y_A, y_C, z_A, z_C)$

$$\partial\phi/\partial x_A = 0,$$

$$\partial\phi/\partial x_C = -\sin\phi/(R\sin\theta),$$

$$\partial\phi/\partial y_A = 0,$$

$$\partial\phi/\partial y_C = \cos\phi/(R\sin\theta),$$

$$\partial\phi/\partial z_A = 0,$$

$$\partial\phi/\partial z_C = 0,$$

$$\partial\theta/\partial x_A = 0,$$

$$\partial\theta/\partial x_C = \cos\phi\cos\theta/R,$$

$$\partial\theta/\partial y_A = 0,$$

$$\partial\theta/\partial y_C = \cos\theta\sin\phi/R,$$

$$\partial\theta/\partial z_A = 0,$$

$$\partial\theta/\partial z_C = -\sin\theta/R,$$

$$\partial\psi/\partial x_A = -(\cos\psi\sin\phi + \cos\phi\cos\theta\sin\psi)/(r\sin\tau),$$

$$\partial\psi/\partial x_C = (\cos\theta\sin\phi\sin\tau + \cos\psi\cos\tau\sin\phi\sin\theta + \cos\phi\cos\tau\cos\theta\sin\psi\sin\theta)(R\sin\tau\sin\theta)^{-1},$$

$$\partial\psi/\partial y_A = (\cos\phi\cos\psi - \cos\theta\sin\phi\sin\psi)(r\sin\tau)^{-1},$$

$$\partial\psi/\partial y_C = -(\cos\phi\cos\theta\sin\tau + \cos\phi\cos\psi\cos\tau\sin\theta - \cos\tau\cos\theta\sin\phi\sin\psi\sin\theta)(R\sin\tau\sin\theta)^{-1},$$

$$\partial\psi/\partial z_A = \sin\psi\sin\theta/(r\sin\tau),$$

$$\partial\psi/\partial z_C = -\cos\tau\sin\psi\sin\theta/(R\sin\tau),$$

$$\partial r/\partial x_A = \cos\phi\cos\tau\sin\theta - \sin\phi\sin\psi\sin\tau + \cos\phi\cos\psi\cos\theta\sin\tau,$$

$$\partial r/\partial x_C = 0,$$

$$\partial r/\partial y_A = \cos\phi\sin\psi\sin\tau + \cos\tau\sin\phi\sin\theta + \cos\psi\cos\theta\sin\phi\sin\tau,$$

$$\partial r/\partial y_C = 0,$$

$$\partial r/\partial z_A = \cos\tau\cos\theta - \cos\psi\sin\tau\sin\theta,$$

$$\partial r/\partial z_C = 0,$$

$$\partial R/\partial x_A = 0,$$

$$\partial R/\partial x_C = \cos\phi\sin\theta,$$

$$\partial R/\partial y_A = 0,$$

$$\partial R/\partial y_C = \sin\phi\sin\theta,$$

$$\partial R/\partial z_A = 0,$$

$$\partial R/\partial z_C = \cos\theta,$$

$$\partial\tau/\partial x_A = [-\cos\tau(\sin\phi\sin\psi - \cos\phi\cos\psi\cos\theta) + \cos\phi\sin\tau\sin\theta]/r,$$

$$\partial\tau/\partial x_C = (\sin\phi\sin\psi - \cos\phi\cos\psi\cos\theta)/R,$$

$$\partial\tau/\partial y_A = [\cos\tau(\cos\phi\sin\psi + \cos\psi\cos\theta\sin\phi) - \sin\phi\sin\tau\sin\theta]/r,$$

$$\partial\tau/\partial y_C = -(\cos\phi\sin\psi + \cos\psi\cos\theta\sin\phi)/R,$$

$$\partial\tau/\partial z_A = -(\cos\theta\sin\tau + \cos\psi\cos\tau\sin\theta)/r,$$

$$\partial\tau/\partial z_C = \cos\psi\sin\theta/R.$$

Appendix B

Proof that two successive transformations $x \to x'$ and $x' \to x''$ are equivalent to the net transformation $x \to x''$

In this appendix it is proved that the transformed Hamiltonian obtained from two successive transformations is equivalent to that obtained from the net transformation. The transformations shall be denoted by the subscript 1 for the first transformation, $x \to x'$, the subscript 2 for the second transformation, $x' \to x''$, and no subscript for the total transformation, $x \to x''$. The Einstein

summation convention is employed, and the sums extend over all degrees of freedom involved in the point transformations.

In the point transformation method, under two successive point transformations, the original Hamiltonian,

$$H(x, \boldsymbol{p}) = p_i p_i + V(\boldsymbol{x}, \boldsymbol{p}), \tag{B.1}$$

is transformed under $\boldsymbol{x} \to \boldsymbol{x}'$ into

$$H(\boldsymbol{x}', \boldsymbol{p}') = p_i(\boldsymbol{x}', \boldsymbol{p}')p_i(\boldsymbol{x}', \boldsymbol{p}') + V[\boldsymbol{x}(\boldsymbol{x}'), \boldsymbol{p}(\boldsymbol{x}', \boldsymbol{p}')], \tag{B.2}$$

and then under $\boldsymbol{x}' \to \boldsymbol{x}''$ into

$$H(\boldsymbol{x}'', \boldsymbol{p}'') = p_i(\boldsymbol{x}'', \boldsymbol{p}'')p_i(\boldsymbol{x}'', \boldsymbol{p}'') + V[\boldsymbol{x}'(\boldsymbol{x}''), \boldsymbol{p}(\boldsymbol{x}'', \boldsymbol{p}'')]. \tag{B.3}$$

Now under the first transformation, $\boldsymbol{x} \to \boldsymbol{x}'$,

$$p_i = p_j'(\partial x_j'/\partial x_i) + (\partial x_j'/\partial x_i)p_j', \tag{B.4}$$

which can be rewritten as [26, 27],

$$p_i = [p_j' + (i\hbar/2)(\partial \ln B_1/\partial x_j')](\partial x_j'/\partial x_i) \tag{B.5}$$

or

$$p_i = (\partial x_k'/\partial x_i)[p_k' - (i\hbar/2)(\partial \ln B_1/\partial x_k')]. \tag{B.6}$$

A similar set of equations, for the second transformation, exists for p_j' in terms of p_l'' and x_l''.

Using Eq. (B.5), and its equivalent equation for the second transformation, one obtains

$$p_i = [p_l'' + (i\hbar/2)(\partial \ln B/\partial x_l'')](\partial x_l''/\partial x_i), \tag{B.7}$$

where the relation $B = B_1 B_2$ has been used. Similarly one can show that

$$p_i = (\partial x_k''/\partial x_i)[p_k'' - (i\hbar/2)(\partial \ln B/\partial x_k'')]. \tag{B.8}$$

Therefore, substituting Eqs. (B.7) and (B.8) into Eq. (B.3), and using the definitions

$$g^{lk} = (\partial x_l''/\partial x_m)(\partial x_k''/\partial x_m) = (\partial x_l/\partial x_i')g_1^{ij}(\partial x_k''/\partial x_j') \tag{B.9}$$

and

$$W(\boldsymbol{x}'') = (\hbar^2/2)B^{1/2}(\partial/\partial x_j'')[g^{ij}(\partial B^{-1/2}/\partial x_j'')], \tag{B.10}$$

one obtains

$$H(\boldsymbol{x}'', \boldsymbol{p}'') = \boldsymbol{p}_l'' g^{lk} \boldsymbol{p}_k'' + W(\boldsymbol{x}'') + V(\boldsymbol{x}'', \boldsymbol{p}''). \tag{B.11}$$

While the above is useful, when the individual transformations are actually done, one first obtains $W_1(\boldsymbol{x}')$ for $\boldsymbol{x} \to \boldsymbol{x}'$, and then $W_2(\boldsymbol{x}'')$ for $\boldsymbol{x}' \to \boldsymbol{x}''$. It shall now be shown that $W(\boldsymbol{x}'')$ is simply equal to the sum of W_1 and W_2.

From Eq. (B.10), W can be rewritten in the form

$$W = -(\hbar^2/2)(\partial/\partial x_i'')[g^{ij}(\partial \ln B/\partial x_j'')] + (\hbar^2/4)(\partial \ln B/\partial x_k'')g^{kl}(\partial \ln B/\partial x_l''), \tag{B.12}$$

or expanding using $B = B_1 B_2$ and $g^{ij} = g_2^{ij}$,

$$W = W_2 - (\hbar^2/2)(\partial/\partial x_i'')[g^{ij}(\partial \ln B_1/\partial x_j'')] + (\hbar^2/4)(\partial \ln B_1/\partial x_m)(\partial \ln B_1/\partial x_m) + (\hbar^2/2)(\partial \ln B_1/\partial x_m)(\partial \ln B_2/\partial x_m). \tag{B.13}$$

Substituting Eq. (B.9), into the first term, and using

$$(\partial/\partial x_i'')(\partial x_i''/\partial x_k') = \partial \ln B_2/\partial x_k', \tag{B.14}$$

one obtains

$$(\partial/\partial x_i'')[g^{ij}(\partial \ln B_1/\partial x_j'')] = (\partial/\partial x_i'')[g_1^{kl}(\partial \ln B_1/\partial x_l')(\partial x_i''/\partial x_k')] = (\partial \ln B_2/\partial x_k')g_1^{kl}(\partial \ln B_1/\partial x_l') + (\partial/\partial x_k')[g_1^{kl}(\partial \ln B_1/\partial x_l)]. \tag{B.15}$$

Substituting this result into Eq. (B.13) and using the form of Eq. (B.12) for the first transformation yields the desired result,

$$W = W_1 + W_2. \tag{B.16}$$

References

1. (a) Zhang JZH, Kouri DJ, Haug K, Schwenke DW, Shima Y, Truhlar DG (1988) J Chem Phys 88:2492–2512; (b) Zhang YC, Zhang JZH, Kouri DJ, Haug K, Schwenke DW, Truhlar DG (1988) Phys Rev Lett 60:2367–2370
2. (a) Miller WH (1969) J Chem Phys 50:407–418; (b) Zhang JZH, Miller WH (1987) Chem Phys Lett 140:329–337; (c) Zhang JZH, Chu SJ, Miller WH (1988) J Chem Phys 6233–6239
3. Kupperman A, Hipes PG (1986) J Chem Phys 84:5962–5964
4. (a) Parker GA, Pack RT, Archer BJ, Walker RB (1987) Chem Phys Lett 137:564–568; (b) Pack RT, Parker GA (1987) J Chem Phys 87:3888–3921
5. Schatz GC, Kupperman A (1976) J Chem Phys 65:4668–4692
6. (a) Webster F, Light JC (1989) J Chem Phys 90:265–299; (b) Ibid: 300–321; (c) Webster F, Light JC (1988) J Chem Phys 85:4744–4745; (d) Walker RB, Stechel EB, Light JC (1978) J Chem Phys 69:2922–2923
7. (a) Redmon MJ, Wyatt RE (1979) Chem Phys Lett 63:209–212; (b) Elkowitz AB, Wyatt RE (1975) J Chem Phys 63:702–721
8. Eyring H, Polanyi JC (1931) Z Phys Chem, Abt B 12:279–311
9. Feynman RP, Hibbs AR (1965) Quantum mechanics and path integrals. McGraw-Hill, New York
10. Miller WH, Hardy NC, Adams JE (1980) J Chem Phys 72:99–112
11. Smith FT (1980) Phys Rev Lett 45:1157–1160
12. Wallace R (1984) Chem Phys 88:247–260
13. Light JC (1971) Adv Chem Phys 19:1–32
14. Mittleman MH (1961) Phys Rev 122:1930–1931
15. Fischer SF, Ratner MA (1972) J Chem Phys 57:2769–2776
16. Witriol NM, Stettler JD, Ratner MA, Sabin JR, Trickey SB (1977) J Chem Phys 66:1141–1159
17. Marcus RA (1968) J Chem Phys 49:2610–2631
18. Hofacker GL, Levine RD (1971) Chem Phys Lett 9:617–620
19. Marcus RA (1966) J Chem Phys 45:4493–4499
20. Child MS (1968) Proc Roy Soc A 292:272–287
21. McNutt JF, Wyatt RE (1979) J Chem Phys 70:5307–5312
22. Davydov AS (1965) Quantum mechanics. Addison-Wesley, Reading

23. (a) Smith FT (1962) J Math Phys 3:735–748; (b) Whitten RC, Smith FT (1968) J Math Phys 9:1103–1113; (c) Whitten RC (1969) J Math Phys 10:1631–1634
24. (a) Johnson BR (1980) J Chem Phys 70:5051–5058; (b) Johnson BR (1983) J Chem Phys 79:1906–1915; (c) Ibid:1916–1925
25. Neumark DM, Wodtke AM, Robinson GN, Heyden CC, Lee YT (1985) J Chem Phys 82:3045–3066
26. Witriol NM (1975) Found Phys 5:591–605
27. Eger M, Gross EP (1963) Ann Phys 24:63–88
28. Wilson EB, Decius JC, Cross C (1955) Molecular vibrations. McGraw-Hill, New York
29. Kemble EC (1937) Fundamental principles of quantum mechanics. McGraw-Hill, New York
30. Podolsky B (1928) Phys Rev 32:812–816
31. Inference Corp (1983) SMP: A symbolic manipulation program
32. Anderson JB (1980) Adv Chem Phys XLI. In Prigogine I, Rice SA (eds). Wiley, New York
33. Levine RD, Bernstein RB (1987) Molecular reaction dynamics. Oxford University Press, New York
34. Connor JNL, Jakubetz W, Manz J (1978) Mol Phys 35:1301–1323
35. Shan Y, Choi BH, Poe RT (1978) Chem Phys Lett 57:379–384
36. Zhang JZH, Miller WH (1988) J Chem Phys 88:4549–4550
37. Launay JM, Lepetit B (1988) Chem Phys Lett 144:346–352
38. Murrell JN, Carter S, Farantos SC, Huxley P, Varandas AJC (1984) Molecular potential energy functions. Wiley, Chichester
39. Stechel EB, Webster F, Light JC (1988) J Chem Phys 88:1824–1827
40. Marcus RA (1968) J Chem Phys 49:2610–2616